WHAT CAN WE LEARN FROM THE STUDY OF SINGLE DIFFRACTIVE DISSOCIATION AT HIGH ENERGIES?*

A.A. Arkhipov
Institute for High Energy Physics
Protvino, 142284 Moscow Region, Russia

Abstract

The fundamental relations in the dynamics of single diffraction dissociation and elastic scattering at high energies are discussed.

PACS numbers: 11.80.-m, 13.85.-t, 21.30.+y
Keywords: inclusive reactions, diffraction dissociation, three-body forces, elastic scattering, total cross-sections, slope of diffraction cone, numeric calculations, fit to the data, interpretation of experiments.

1 Introduction

I shall start my talk from the end with the short answer to the question in the title. The study of the inclusive reactions in the region of diffraction dissociation at high energies provides a unique possibility to learn on a new type of interactions between elementary particles or a new type of fundamental forces, which the three-body forces are. What was the beginning on?

In 1994 the CDF group at Fermilab published new results on the measurements of $p\bar{p}$ single diffraction dissociation at $\sqrt{s} = 546$ and 1800 GeV. They observed that a popular supercritical Pomeron model did not describe

*The talk presented at the VIIIth Blois Workshop on Elastic and Diffractive Scattering. Protvino, Russia, June 28–July 2, 1999.

new measured values. The statement, made in [1], is as follows: The value of $\sigma_{sd}^{p\bar{p}} = (7.89 \pm 0.33)\ mb$, measured at $\sqrt{s} = 546\ GeV$, is extrapolated by the supercritical Pomeron model to $\sigma_{sd}^{p\bar{p}} = (13.9 \pm 0.9)\ mb$ at $\sqrt{s} = 1800\ GeV$, while the measured value at this energy is equal to $\sigma_{sd}^{p\bar{p}} = (9.45 \pm 0.44)\ mb$. The ratio of the measured $\sigma_{sd}^{p\bar{p}}$ to that obtained by extrapolation is

$$\frac{\sigma_{sd}^{p\bar{p}}(experimental)}{\sigma_{sd}^{p\bar{p}}(extrapolation)}(\sqrt{s} = 1800\ GeV) = 0.68 \pm 0.05. \qquad (1)$$

Moreover, at $\sqrt{s} = 20\ GeV$ the experimental $\sigma_{sd}^{p\bar{p}} = (4.9 \pm 0.55)\ mb$ is 4.5 times larger than the value $\sigma_{sd}^{p\bar{p}} = (1.1 \pm 0.17)\ mb$, obtained by the extrapolation of the measured value of $\sigma_{sd}^{p\bar{p}}$ at $\sqrt{s} = 546\ GeV$ down to $\sqrt{s} = 20\ GeV$ with the help of the supercritical Pomeron model. So, the latest experimental measurement of $p\bar{p}$ single diffraction dissociation at c.m.s. energies $\sqrt{s} = 546$ and $1800\ GeV$, carried out by the CDF group at the Fermilab Tevatron collider, has shown that the popular model of supercritical Pomeron does not describe the existing experimental data.

We called the emerged situation as a supercrisis for the supercritical Pomeron model (SCPM).[1] The supercrisis is illustrated on Fig. 1 extracted from paper [3].

The attempts undertaken in Refs. [3, 4] to save the SCPM are also shown on this figure. Unfortunately GLM paper [4] contains a crude mathematical mistake. The mistake was observed by B.V. Struminsky and E.S. Martynov from Kiev [5]. Besides, in our opinion, an eikonalization procedure cannot be considered as a saving ring for SCPM because this procedure is outside the original Regge ideology. The idea of renormalized Pomeron flux proposed by Goulianos is a good physical idea for an experimentalist, but this idea cannot be a satisfactory one for a theorist because the idea is not grounded by the underlying Regge theory.

Obviously, the foundations of the Pomeron model require a further theoretical study and the construction of newer, more general phenomenological framework, which would enable one to remove the discrepancy between the model predictions and the experiment.

Although nowadays we have in the framework of local quantum field theory a gauge model of strong interactions formulated in terms of the known

[1] Recent experimental results from HERA [2] lead us to the same conclusion. The soft Pomeron phenomenology as currently developed cannot incorporate the HERA data on structure function F_2 at small x and total $\gamma^* p$ cross section from F_2 measurements as a function of W^2 for different Q^2.

QCD Lagrangian, its relations to the so called "soft" (interactions at large distances) hadronic physics are far from desired. The understanding of this physics is high interest because it has an intrinsically fundamental nature.

In 1970 the experiments at the Serpukhov accelerator revealed that the K^+p total cross section increased with energy. The increase of the pp total cross section was discovered at the CERN ISR and then the effect of rising total cross sections was confirmed at the Fermilab accelerator.

In spite of more than 25 years after the formulation of QCD we still cannot obtain from the QCD Lagrangian the answer to the question why all the hadronic total cross-sections grow with energy. We cannot predict total cross-sections in an absolute way starting from the fundamental QCD Lagrangian as well mainly because it is not a perturbative problem.

It is well known, e.g., that nonperturbative contributions to the gluon propagator influence the behaviour of "soft" hadronic processes and the knowledge of the infrared behaviour of QCD is certainly needed to describe the "soft" hadronic physics in the framework of QCD. Unfortunately, today we don't know the whole picture of the infrared behaviour of QCD, we have some fragments of this picture though (see e.g. Ref. [6]).

At the same time it is more or less clear now that the rise of the total cross-sections is just the shadow (not antishadow!) of particle production.

Through the optical theorem the total cross-section is related to the imaginary part of the elastic scattering amplitude in the forward direction. That is why the theoretical understanding of elastic scattering has the fundamental importance.

From the unitarity relation it follows that the imaginary part of the elastic scattering amplitude contains the contribution of all possible inelastic channels in two-particle interaction. It is clear therefore that we cannot understand the elastic scattering without understanding the inelastic interaction.

Among all the possible inelastic interactions there is a special class of processes which are called a single diffraction dissociation. The single diffraction dissociation is the scattering process where one of two particles in the initial state breaks up during the interaction producing a system of particles in a limited region of (pseudo)rapidity.[2]

[2]Pseudorapidity is defined as $\eta = -\ln\tan(\theta/2)$ where θ is the polar angle of the produced particle with respect to the beam direction. Pseudorapidity is frequently used as an approximation to rapidity.

Good and Walker have shown [7] that the single diffraction dissociation is predicted by the basic principles of quantum mechanics. However both the elastic scattering and single diffraction dissociation cannot correctly be calculated in QCD due to the non-perturbative nature of the interactions.

The popular Regge phenomenology represents elastic and diffractive scattering by the exchange of the Pomeron, a color singlet Reggeon with quantun numbers of the vacuum. It should be noted that the definition of the Pomeron as Reggeon with the highest Regge trajectory $\alpha_P(t)$, carrying the quantum numbers of the vacuum, is not the only one.[3] There are many other definitions of the Pomeron: Pomeron is a gluon "ladder" [8]; Pomeron is a bound state of two reggezied gluons – BFKL-Pomeron [9]; soft and hard Pomerons [10, 11]; etc.[4] This leapfrog is because of the exact nature of the Pomeron and its detailed substructure remains such as that no one knows what it is. The difficulty of establishing the true nature of the Pomeron in QCD is almost obviously related to the calculations of non-perturbative gluon exchange.

Nevertheless in the near past simple formulae of the Regge phenomenology provided good parameterization of experimental data on "soft" hadronic physics and pragmatic application of Pomeron phenomenology had been remarkably successful (see e.g. the latest issue of the Review of Particles Properties).

That was the case before the appearance of the above-mentioned CDF data on single diffractive dissociation and recent results from HERA. Of course, it is good that we have a simple and compact form for representing a great variety of data for different hadronic processes, but it is certainly bad that power behaved total cross-sections violate unitarity. Often and often encountered claim, that the model with power behaved total cross-sections is valid in the non-asymptotic domain which has been explored up today, is not correct because the supercritical Pomeron model is an asymptotic one by definition.

We suggested another approach to the dynamical description of one-particle inclusive reactions [12]. The main point of our approach is that new fundamental three-body forces are responsible for the dynamics of particle production processes of inclusive type. Our consideration revealed several fundamental properties of one-particle inclusive cross-sections in the region

[3]For supercritical Pomeron $\alpha_P(0) - 1 = \Delta \ll 1$, $\Delta > 0$ is responsible for the growth of hadronic cross-sections with energy.

[4]At the Workshop I heard new definition of Pomeron from N.N. Nikolaev: Pomeron is (neither more nor less!) a label of diffraction.

of diffraction dissociation. In particular, it was shown that the slope of the diffraction cone in $p\bar{p}$ single diffraction dissociation is related to the effective radius of three-nucleon forces in the same way as the slope of the diffraction cone in elastic $p\bar{p}$ scattering is related to the effective radius of two-nucleon forces. It was also demonstrated that the effective radii of two- and three-nucleon forces, which are the characteristics of elastic and inelastic interactions of two nucleons, define the structure of the $p\bar{p}$ total cross-sections in a simple and physically clear form. I'll touch upon these properties later on.

First of all let me tell you a few words what I mean by three-body forces about.

2 Three-body forces in relativistic quantum theory

Using the LSZ or the Bogoljubov reduction formulae in quantum field theory [13] we can easily obtain the following cluster structure for $3 \to 3$ scattering amplitude (see diagram below)

$$\mathcal{F}_{123} = \mathcal{F}_{12} + \mathcal{F}_{23} + \mathcal{F}_{13} + \mathcal{F}^C_{123} \tag{2}$$

where $\mathcal{F}_{ij}, (i,j = 1,2,3)$ are $2 \to 2$ scattering amplitudes, $\mathcal{F}^C_{123}$ is called the connected part of the $3 \to 3$ scattering amplitude.

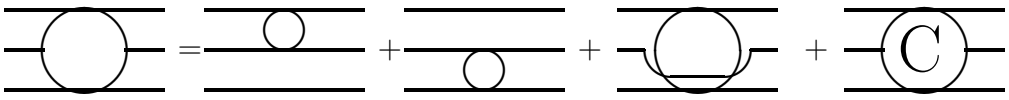

In the framework of single-time formalism in quantum field theory [14] we construct the $3 \to 3$ off energy shell scattering amplitude $T_{123}(E)$ with the same (cluster) structure as (2)

$$T_{123}(E) = T_{12}(E) + T_{23}(E) + T_{13}(E) + T^C_{123}(E). \tag{3}$$

Following the tradition we'll call the kernel describing the interaction of three particles as the three particle interaction quasipotential. The three particle interaction quasipotential $V_{123}(E)$ is related to the off-shell $3 \to 3$ scattering amplitude $T_{123}(E)$by the Lippmann-Schwinger type equation

$$T_{123}(E) = V_{123}(E) + V_{123}(E)G_0(E)T_{123}(E). \tag{4}$$

There exists the same transformation between two particle interaction quasipotentials V_{ij} and off energy shell $2 \to 2$ scattering amplitudes T_{ij}

$$T_{ij}(E) = V_{ij}(E) + V_{ij}(E)G_0(E)T_{ij}(E). \tag{5}$$

It can be shown that in the quantum field theory the three particle interaction quasipotential has the following structure [15]

$$V_{123}(E) = V_{12}(E) + V_{23}(E) + V_{13}(E) + V_0(E). \tag{6}$$

The quantity $V_0(E)$ is called the three-body forces quasipotential. The $V_0(E)$ represents the defect of three particle interaction quasipotential over the sum of two particle interaction quasipotentials and describes the true three-body interactions. The three-body forces quasipotential is an inherent connected part of total three particle interaction quasipotential which cannot be represented by the sum of pair interaction quasipotentials.

The three-body forces scattering amplitude is related to the three-body forces quasipotential by the equation

$$T_0(E) = V_0(E) + V_0(E)G_0(E)T_0(E). \tag{7}$$

It should be stressed that the three-body forces appear as a result of consistent consideration of three-body problem in the framework of local quantum field theory.

3 Global analyticity of the three-body forces

Let us introduce the following useful notations

$$< p_1' p_2' p_3' | S - 1 | p_1 p_2 p_3 >= 2\pi i \delta^4 (\sum_{i=1}^{3} p_i' - \sum_{j=1}^{3} p_j) \mathcal{F}_{123}(s; \hat{e}', \hat{e}), \tag{8}$$

$$s = (\sum_{i=1}^{3} p_i')^2 = (\sum_{j=1}^{3} p_j)^2.$$

The $\hat{e}', \hat{e} \in S_5$ are two unit vectors on five-dimensional sphere describing the configuration of three-body system in the initial and final states (before and after scattering).

We will denote the quantity T_0 restricted on the energy shell as

$$T_0 \mid_{on\, energy\, shell} = \mathcal{F}_0.$$

The unitarity condition for the quantity $\mathcal{F}_0$ with account for the introduced notations can be written in form [16, 17]

$$\begin{aligned} & Im\mathcal{F}_0(s;\hat{e}',\hat{e}) = \\ & = \pi A_3(s) \int d\Omega_5(\hat{e}'')\mathcal{F}_0(s;\hat{e}',\hat{e}'') \overset{*}{\mathcal{F}}_0 (s;\hat{e},\hat{e}'') + H_0(s;\hat{e}',\hat{e}), \end{aligned} \tag{9}$$

$$Im\mathcal{F}_0(s;\hat{e}',\hat{e}) = \frac{1}{2i}\left[\mathcal{F}_0(s;\hat{e}',\hat{e}) - \overset{*}{\mathcal{F}}_0 (s;\hat{e},\hat{e}')\right],$$

where

$$A_3(s) = \Gamma_3(s)/S_5,$$

$\Gamma_3(s)$ is the three-body phase-space volume, S_5 is the volume of unit five-dimensional sphere. H_0 defines the contribution of all the inelastic channels emerging due to three-body forces.

Let us introduce a special notation for the scalar product of two unit vectors $\hat{e}'$ and $\hat{e}$

$$\cos\omega = \hat{e}^{'} \cdot \hat{e}. \tag{10}$$

We will use the other notation for the three-body forces scattering amplitude as well

$$\mathcal{F}_0(s;\hat{e}',\hat{e}) = \mathcal{F}_0(s;\eta,\cos\omega),$$

where all other variables are denoted through η.

Now we are able to go to the formulation of our basic assumption on the analytical properties for the three-body forces scattering amplitude [16, 17].

We will assume that for physical values of the variable s and fixed values of η the amplitude $\mathcal{F}_0(s;\eta,\cos\omega)$ is an analytical function of the variable $\cos\omega$ in the ellipse $E_0(s)$ with the semi-major axis

$$z_0(s) = 1 + \frac{M_0^2}{2s} \tag{11}$$

and for any $\cos\omega \in E_0(s)$ and physical values of η it is polynomially bounded in the variable s. M_0 is some constant having mass dimensionality.

Such analyticity of the three-body forces amplitude was called a global one. The global analyticity may be considered as a direct geometric generalization of the known analytical properties of two-body scattering amplitude strictly proved in the local quantum field theory [18, 19, 20, 21, 22].

At the same time the global analyticity results in the generalized asymptotic bounds.

GLOBAL ANALYTICITY & **UNITARITY**

$$\Downarrow$$

GENERALIZED ASYMPTOTIC BOUNDS

For example the generalized asymptotic bound for $O(6)$-invariant three-body forces scattering amplitude looks like [16, 17]

$$Im\,\mathcal{F}_0(s;...) \leq \mathrm{Const}\, s^{3/2}(\frac{\ln s/s_0'}{M_0})^5 = \mathrm{Const}\, s^{3/2} R_0^5(s), \tag{12}$$

where $R_0(s)$ is the effective radius of the three-body forces introduced according to [22] where the effective radius of two-body forces has been defined,

$$R_0(s) = \frac{\Lambda_0}{\Pi(s)} = \frac{r_0}{M_0}\ln\frac{s}{s_0'}, \quad \Pi(s) = \frac{\sqrt{s}}{2}, \quad s \to \infty, \tag{13}$$

r_0 is defined by the power of the amplitude $\mathcal{F}_0$ growth at high energies [17], M_0 defines the semi-major axis of the global analyticity ellipse (11), Λ_0 is the effective global orbital momentum, $\Pi(s)$ is the global momentum of three-body system, s_0' is a scale defining unitarity saturation of three-body forces.

It is well known that the Froissart asymptotic bound [23] can be experimentally verified, because with the help of the optical theorem we can connect the imaginary part of $2 \to 2$ scattering amplitude with the experimentally measurable quantity which is the total cross-section. So, if we want to have a possibility for the experimental verification of the generalized asymptotic bounds ($n \geq 3$), we have to establish a connection between the many-body forces scattering amplitudes and the experimentally measurable quantities. For this aim we have considered the problem of high energy particle scattering from deuteron and on this way we found the connection of the three-body forces scattering amplitude with the experimentally measurable quantity which is the total cross-section for scattering from deuteron

[24]. Moreover the relation of the three-body forces scattering amplitude to one-particle inclusive cross-sections has been established [25].

I shall briefly sketch now the basic results of our analysis of high-energy particle scattering from deuteron.

4 Scattering from deuteron

The problem of scattering from two-body bound states was treated in [24, 25] with the help of dynamic equations obtained on the basis of single-time formalism in QFT [15]. As has been shown in [24, 25], the total cross-section in the scattering from deuteron can be expressed by the formula

$$\sigma_{hd}^{tot}(s) = \sigma_{hp}^{tot}(\hat{s}) + \sigma_{hn}^{tot}(\hat{s}) - \delta\sigma(s), \tag{14}$$

where $\sigma_{hd}, \sigma_{hp}, \sigma_{hn}$ are the total cross-sections in scattering from deuteron, proton and neutron,

$$\delta\sigma(s) = \delta\sigma_G(s) + \delta\sigma_0(s), \tag{15}$$

$$\delta\sigma_G(s) = \frac{\sigma_{hp}^{tot}(\hat{s})\sigma_{hn}^{tot}(\hat{s})}{4\pi(R_d^2 + B_{hp}(\hat{s}) + B_{hn}(\hat{s}))} \equiv \frac{\sigma_{hp}^{tot}(\hat{s})\sigma_{hn}^{tot}(\hat{s})}{4\pi R_{eff}^2(s)}, \quad \hat{s} = \frac{s}{2}, \tag{16}$$

$B_{hN}(s)$ is the slope of the forward diffraction peak in the elastic scattering from nucleon, $1/R_d^2$ is defined by the deuteron relativistic formfactor

$$\frac{1}{R_d^2} \equiv \frac{q}{\pi}\int \frac{d\vec{\Delta}\Phi(\vec{\Delta})}{2\omega_h(\vec{q}+\vec{\Delta})}\delta\left[\omega_h(\vec{q}+\vec{\Delta}) - \omega_h(\vec{q})\right], \quad \frac{s}{2M_d} \cong q \cong \frac{\hat{s}}{2M_N}, \tag{17}$$

$\delta\sigma_G$ is the Glauber correction or shadow effect. The Glauber shadow correction originates from elastic rescatterings of an incident particle on the nucleons inside the deuteron.

The quantity $\delta\sigma_0$ represents the contribution of the three-body forces to the total cross-section in the scattering from deuteron. The physical reason for the appearance of this quantity is directly connected with the inelastic interactions of an incident particle with the nucleons of deuteron. Paper [25] provides for this quantity the following expression:

$$\delta\sigma_0(s) = -\frac{(2\pi)^3}{q}\int \frac{d\vec{\Delta}\Phi(\vec{\Delta})}{2E_p(\vec{\Delta}/2)2E_n(\vec{\Delta}/2)} Im\, R(s; -\frac{\vec{\Delta}}{2}, \frac{\vec{\Delta}}{2}, \vec{q}; \frac{\vec{\Delta}}{2}, -\frac{\vec{\Delta}}{2}, \vec{q}), \tag{18}$$

where q is the incident particle momentum in the lab system (rest frame of deuteron), $\Phi(\vec{\Delta})$ is the deuteron relativistic formfactor, normalized to unity at zero,

$$E_N(\vec{\Delta}) = \sqrt{\vec{\Delta}^2 + M_N^2} \quad N = p, n,$$

M_N is the nucleon mass. The function R is expressed via the amplitude of the three-body forces T_0 and the amplitudes of elastic scattering from the nucleons T_{hN} by the relation

$$R = T_0 + \sum_{N=p,n} (T_0 G_0 T_{hN} + T_{hN} G_0 T_0). \tag{19}$$

In [24] the contribution of three-body forces to the scattering amplitude from deuteron was related to the processes of multiparticle production in the inelastic interactions of the incident particle with the nucleons of deuteron. This was done with the help of the unitarity equation. The character of the energy dependence of $\delta\sigma_0$ was shown to be governed by the energy behaviour of the corresponding inclusive cross-sections.

Here, for simplicity, let us consider the model where the imaginary part of the three-body forces scattering amplitude has the form

$$Im\,\mathcal{F}_0(s; \vec{p}_1, \vec{p}_2, \vec{p}_3; \vec{q}_1, \vec{q}_2, \vec{q}_3) = f_0(s) \exp\left\{-\frac{R_0^2(s)}{4} \sum_{i=1}^{3} (\vec{p}_i - \vec{q}_i)^2\right\}, \tag{20}$$

where $f_0(s)$, $R_0(s)$ are free parameters which, in general, may depend on the total energy of three-body interaction. Note that the quantity $f_0(s)$ has the dimensionality $[R^2]$.

In case of unitarity saturation of the three-body forces, we have from the generalized asymptotic theorems

$$f_0(s) \sim \mathrm{Const}\, s^{3/2} \Big(\frac{\ln s/s_0'}{M_0}\Big)^5 = \mathrm{Const}\, s^{3/2} R_0^5(s), \tag{21}$$

$$R_0(s) = \frac{r_0}{M_0} \ln s/s_0' \quad s \to \infty. \tag{22}$$

In the model all the integrals can be calculated in the analytical form. As a result, we obtain for the quantity $\delta\sigma_0$ [25]

$$\delta\sigma_0(s) = \frac{(2\pi)^6 f_0(s)}{s M_N} \left\{ \frac{\sigma_{hN}(s/2)}{2\pi[B_{hN}(s/2) + R_0^2(s) - R_0^4(s)/4(R_0^2(s) + R_d^2)]} - 1 \right\}$$

$$\times \frac{1}{[2\pi(R_d^2 + R_0^2(s))]^{3/2}}. \tag{23}$$

If the condition

$$R_0^2(s) \simeq B_{hN}(s/2) \ll R_d^2 \tag{24}$$

is realized, then we obtain from expression (23)

$$\delta\sigma_0(s) = (2\pi)^{9/2} \frac{f_0(s)\chi(s)}{sM_N R_d^3}, \tag{25}$$

where

$$\chi(s) = \frac{\sigma_{hN}^{tot}(s/2)}{2\pi[B_{hN}(s/2) + R_0^2(s)]} - 1, \tag{26}$$

and we suppose that asymptotically

$$B_{hp} = B_{hn} \equiv B_{hN}, \quad \sigma_{hp}^{tot} = \sigma_{hn}^{tot} \equiv \sigma_{hN}^{tot}.$$

It follows from the Froissart theorem and generalized asymptotic bounds (12) that the following asymptotic behaviour is admitted for the $\chi(s)$:

$$\chi(s) \sim \frac{1}{\sqrt{s}\ln^3 s}, \quad s \to \infty. \tag{27}$$

5 Three-body forces in single diffraction dissociation

From the analysis of the problem of high-energy particle scattering from deuteron we have derived the formula connecting one-particle inclusive cross-section with the imaginary part of the three-body forces scattering amplitude. This formula looks like

$$\boxed{2E_N(\vec{\Delta})\frac{d\sigma_{hN\to NX}}{d\vec{\Delta}}(s,\vec{\Delta}) = -\frac{(2\pi)^3}{I(s)} Im\mathcal{F}_0^{scr}(\bar{s};-\vec{\Delta},\vec{\Delta},\vec{q};\vec{\Delta},-\vec{\Delta},\vec{q})}, \tag{28}$$

$$Im\mathcal{F}_0^{scr}(\bar{s};-\vec{\Delta},\vec{\Delta},\vec{q};\vec{\Delta},-\vec{\Delta},\vec{q}) = Im\mathcal{F}_0(\bar{s};-\vec{\Delta},\vec{\Delta},\vec{q};\vec{\Delta},-\vec{\Delta},\vec{q}) -$$

$$-4\pi \int d\vec{\Delta}' \frac{\delta\left[E_N(\vec{\Delta}-\vec{\Delta}') + \omega_h(\vec{q}+\vec{\Delta}') - E_N(\vec{\Delta}) - \omega_h(\vec{q})\right]}{2\omega_h(\vec{q}+\vec{\Delta}')2E_N(\vec{\Delta}-\vec{\Delta}')} \times$$

$$Im\mathcal{F}_{hN}(\hat{s};\vec{\Delta},\vec{q};\vec{\Delta}-\vec{\Delta}',\vec{q}+\vec{\Delta}')Im\mathcal{F}_0(\bar{s};-\vec{\Delta},\vec{\Delta}-\vec{\Delta}',\vec{q}+\vec{\Delta}';\vec{\Delta},-\vec{\Delta},\vec{q}), \quad (29)$$

$$E_N(\vec{\Delta})=\sqrt{\vec{\Delta}^2+M_N^2}, \quad \omega_h(\vec{q})=\sqrt{\vec{q}^2+m_h^2},$$
$$I(s)=2\lambda^{1/2}(s,m_h^2,M_N^2), \quad \hat{s}=\frac{\bar{s}+m_h^2-2M_N^2}{2},$$
$$\bar{s}=2(s+M_N^2)-M_X^2, \quad t=-4\vec{\Delta}^2.$$

I'd like to draw the attention to the minus sign in the R.H.S. of Eq. (28). The simple model for the three-body forces considered above (see Eq. (20)) gives the following result for the one-particle inclusive cross-section in the region of diffraction dissociation

$$\frac{s}{\pi}\frac{d\sigma_{hN\to NX}}{dtdM_X^2}=\frac{(2\pi)^3}{I(s)}\chi(\bar{s})Im\mathcal{F}_0(\bar{s};-\vec{\Delta},\vec{\Delta},\vec{q};\vec{\Delta},-\vec{\Delta},\vec{q})$$
$$=\frac{(2\pi)^3}{I(s)}\chi(\bar{s})f_0(\bar{s})\exp\left[\frac{R_0^2(\bar{s})}{2}t\right] \quad (30)$$

where

$$\chi(\bar{s})=\frac{\sigma_{hN}^{tot}(\bar{s}/2)}{2\pi[B_{hN}(\bar{s}/2)+R_0^2(\bar{s})]}-1.$$

The configuration of particles momenta and kinematical variables are shown in Fig. 2. The variable $\bar{s}$ in the R.H.S. of Eq. (30) is related to the kinematical variables of one-particle inclusive reaction by the equation

$$\bar{s}=2(s+M_N^2)-M_X^2, \quad (31)$$
$$t=-4\Delta^2.$$

There is a temptation to call the quantity $I(s)\chi^{-1}(\bar{s})$ a renormalized flux. However, it should be pointed out that in our case we have a flux of real particles and function $\chi(s)$ has quite a clear physical meaning. The function $\chi(s)$ originates from initial and final states interactions and describes the effect of screening the three-body forces by two-body ones [25].

If we take the usual parameterization for one-particle inclusive cross-section in the region of diffraction dissociation

$$\frac{s}{\pi}\frac{d\sigma}{dtdM_X^2}=A(s.M_X^2)\exp[b(s,M_X^2)t], \quad (32)$$

then we obtain for the quantities A and b

$$A(s,M_X^2)=\frac{(2\pi)^3}{I(s)}\chi(\bar{s})f_0(\bar{s}),\quad b(s,M_X^2)=\frac{R_0^2(\bar{s})}{2}. \tag{33}$$

Eq. (33) shows that the effective radius of three-body forces is related to the slope of diffraction cone for inclusive diffraction dissociation processes in the same way as the effective radius of two-body forces is related to the slope of diffraction cone in elastic scattering processes. Moreover, it follows from the expressions

$$R_0(\bar{s})=\frac{r_0}{M_0}\ln\bar{s}/s_0',\quad \bar{s}=2(s+M_N^2)-M_X^2$$

that the slope of diffraction cone for inclusive diffraction dissociation processes at fixed energy decreases with the growth of missing mass. This property agrees well qualitatively with the experimentally observable picture.

Hence physically tangible notion of the effective radius of three-body forces introduced previously provides a clear physical interpretation that helps one to create a visual picture and representation for inclusive diffraction dissociation processes at the same level as one can understand and represent elastic scattering processes at high energies. Besides, relation (28) together with linear equation (7) for the three-body forces scattering amplitude may be the basis of powerful dynamic apparatus for constructing the dynamical models for the theoretical description of the inclusive reactions.

In the case of unitarity saturation of the three-body forces, we have from generalized asymptotic theorems

$$f_0(s)\sim s^{3/2}\left(\frac{\ln s/s_0'}{M_0}\right)^5,\quad \chi(s)\sim\frac{1}{\sqrt{s}\ln^3 s},\quad s\to\infty.$$

This means that

$$\boxed{A(s,M_X^2)\sim\ln^2\frac{\bar{s}}{s_0'},\quad s\to\infty}. \tag{34}$$

On the other hand, comparing formulae (25) and (33) we see that one and the same combination χf_0 enters in the equations. Therefore, we can extract this combination and express it through experimentally measurable quantities. We have in this way

$$A(s,M_X^2)=\frac{\bar{s}M_N R_d^3}{(2\pi)^{3/2}I(s)}\delta\sigma_0(\bar{s}). \tag{35}$$

In that case it would be very desirable to think about the creation of accelerating deuterons beams instead of protons ones at the now working accelerators and colliders.

6 On the structure of hadronic total cross-sections

Let's rewrite the equation for $\chi(s)$

$$\chi(s) = \frac{\sigma_{hN}^{tot}(s/2)}{2\pi[B_{hN}(s/2) + R_0^2(s)]} - 1$$

in the form

$$\sigma_{hN}^{tot}(s) = 2\pi \left[B_{hN}(s) + R_0^2(2s)\right](1+\chi)\,. \tag{36}$$

From the Froissart and generalized asymptotic bounds we have

$$\chi(s) = O\left(\frac{1}{\sqrt{s}\ln^3 s}\right), \quad s \to \infty.$$

We also know that [20]

$$\sigma_{hN}^{tot}(s, s_0) \sim \ln^2(s/s_0) \Longrightarrow B_{hN}(s, s_0) \sim \ln^2(s/s_0), \tag{37}$$

and Eq. (36) gives

$$R_0^2(2s, s_0') \sim \ln^2(2s/s_0') \sim \ln^2(s/s_0), \quad s \to \infty.$$

Therefore, we come to the following asymptotic consistency condition:

$$\boxed{s_0' = 2s_0}\,. \tag{38}$$

The asymptotic consistency condition tells us that we have not any new scale. The scale defining unitarity saturation of three-body forces is unambiguously expressed by the scale which defines unitarity saturation of two-body forces. In that case we have

$$R_0^2(2s, s_0') = R_0^2(s, s_0)$$

and

$$\boxed{\sigma_{hN}^{tot}(s) = 2\pi \left[B_{hN}(s) + R_0^2(s)\right](1+\chi(s))} \tag{39}$$

with a common scale s_0.

Reminding the relation between the effective radius of two-body forces and the slope of diffraction cone in elastic scattering

$$B_{hN}(s) = \frac{1}{2} R^2_{hN}(s), \tag{40}$$

we obtain

$$\sigma^{tot}_{hN}(s) = \pi R^2_{hN}(s) + 2\pi R^2_0(s), \quad s \to \infty. \tag{41}$$

Equations (39) and (41) define a new nontrivial structure of hadronic total cross-section. It should be emphasized that the coefficients staying in the R.H.S. of Eq. (41) in front of effective radii of two- and three-body forces are strongly fixed.

It is useful to compare the new structure of total hadronic cross-section with the known structure. We have from unitarity

$$\sigma^{tot}_{hN}(s) = \sigma^{el}_{hN}(s) + \sigma^{inel}_{hN}(s). \tag{42}$$

If we put

$$\sigma^{el}_{hN}(s) = \pi R^{el\,2}_{hN}(s), \quad \sigma^{inel}_{hN}(s) = 2\pi R^{inel\,2}_{hN}(s), \tag{43}$$

then we come to the similar formula

$$\sigma^{tot}_{hN}(s) = \pi R^{el\,2}_{hN}(s) + 2\pi R^{inel\,2}_{hN}(s). \tag{44}$$

But it should be borne in mind

$$R^2_{hN}(s) \neq R^{el\,2}_{hN}(s), \quad R^2_0(s) \neq R^{inel\,2}_{hN}(s). \tag{45}$$

In fact, we have

$$\sigma^{el}_{hN}(s) = \frac{\sigma^{tot\,2}_{hN}(s)}{16\pi B_{hN}(s)} = \frac{\sigma^{tot\,2}_{hN}(s)}{8\pi R^2_{hN}(s)}, \tag{46}$$

$$\sigma^{inel}_{hN}(s) = \sigma^{tot}_{hN}(s) \left[1 - \frac{\sigma^{tot}_{hN}(s)}{8\pi R^2_{hN}(s)} \right]. \tag{47}$$

Of course, Eqs. (43) are the definitions of R^{el}_{hN} and R^{inel}_{hN}. The definition of R^{el}_{hN} corresponds to our classical imagination, the definition of R^{inel}_{hN} corresponds to our knowledge of quantum mechanical problem for scattering from the black disk. Let us suppose that

$$\sigma^{tot}_{hN}(s_m) \cong \pi R^2_{hN}(s_m), \quad s_m \in \mathcal{M}, \quad \left(R^2_0(s_m) \ll R^2_{hN}(s_m) \right), \tag{48}$$

then we obtain

$$\sigma_{hN}^{el}(s_m) = \frac{1}{8}\pi R_{hN}^2(s_m), \quad \sigma_{hN}^{inel}(s_m) = \frac{7}{8}\pi R_{hN}^2(s_m). \tag{49}$$

This simple example shows that the new structure of total hadronic cross-sections is quite different from that given by Eq. (42). The reason is that the structure (39) is of the dynamical origin. We have mentioned above that the coefficients, staying in the R.H.S. of Eq. (41) in front of effective radii of two- and three-body forces, are strongly fixed. In fact, we found here the answer to the old question: Why the constant ($\pi/m_\pi^2 \approx 60\,mb$) staying in the Froissart bound is too large in the light of the existing experimental data. The constant in the R.H.S. of Eq. (41), staying in front of effective radius of hadron-hadron interaction, is 4 times smaller than the constant in the Froissart bound. But this is too small to correspond to the experimental data. The second term in the R.H.S. of Eq. (41) fills an emerged gap.

It is a remarkable fact that the quantity R_0^2, which has the clear physical interpretation, at the same time, is related to the experimentally measurable quantity which the total cross-section is. This important circumstance gives rise to the new nontrivial consequences which are discussed in the next section.

We made an attempt to check up the structure (39) on its correspondence to the existing experimental data and I'd like to present the preliminary results here.

At the first step, we made a weighted fit to the experimental data on the proton-antiproton total cross-sections in the range $\sqrt{s} > 10\,GeV$. The data were fitted with the function of the form predicted by Froissart bound in the spirit of our approach[5]

$$\sigma_{asmpt}^{tot} = a_0 + a_2 \ln^2(\sqrt{s}/\sqrt{s_0}) \tag{50}$$

where $a_0, a_2, \sqrt{s_0}$ are free parameters. We accounted for experimental errors δx_i (statistical and systematic errors added in quadrature) by fitting to the experimental points with the weight $w_i = 1/(\delta x_i)^2$. Our fit yielded

$$a_0 = (42.0479 \pm 0.1086)mb, \quad a_2 = (1.7548 \pm 0.0828)mb, \tag{51}$$

[5]Recently, from a careful analysis of the experimental data and a comparative study of the known characteristic parameterizations, Bueno and Velasco have shown (Phys. Lett. B**380**, 184 (1996)) that statistically a "Froissart-like" type parameterization for proton-proton and proton-antiproton total cross-sections is strongly favoured.

$$\sqrt{s_0} = (20.74 \pm 1.21) GeV. \tag{52}$$

The fit result is shown in Fig. 3.

After that we made a weighted fit to the experimental data on the slope of diffraction cone in elastic $p\bar{p}$ scattering. The experimental points and the references, where they have been extracted from, are listed in [26]. The fitted function of the form

$$B = b_0 + b_2 \ln^2(\sqrt{s}/20.74), \tag{53}$$

which is also suggested by the asymptotic theorems of local quantum field theory, has been used. The value $\sqrt{s_0}$ has been fixed by (52) from the fit to the $p\bar{p}$ total cross-sections data. Our fit yielded

$$b_0 = (11.92 \pm 0.15) GeV^{-2}, \quad b_2 = (0.3036 \pm 0.0185) GeV^{-2}. \tag{54}$$

The fitting curve is shown in Fig. 4.

At the final stage we build a global (weighted) fit to all the data on proton-antiproton total cross-sections in a whole range of energies available up today. The global fit was made with the function of the form

$$\sigma^{tot}_{p\bar{p}}(s) = \sigma^{tot}_{asmpt}(s) \left[1 + \frac{c}{\sqrt{s - 4m_N^2} R_0^3(s)} \left(1 + \frac{d_1}{\sqrt{s}} + \frac{d_2}{s} + \frac{d_3}{s^{3/2}} \right) \right] \tag{55}$$

where m_N is proton (nucleon) mass,

$$R_0^2(s) = \left[0.40874044 \sigma^{tot}_{asmpt}(s)(mb) - B(s) \right] (GeV^{-2}), \tag{56}$$

$$\sigma^{tot}_{asmpt}(s) = 42.0479 + 1.7548 \ln^2(\sqrt{s}/20.74), \tag{57}$$

$$B(s) = 11.92 + 0.3036 \ln^2(\sqrt{s}/20.74), \tag{58}$$

c, d_1, d_2, d_3 are free parameters. Function (55) corresponds to the structure given by Eq. (39).

In fact, we have for the function $\chi(s)$ in the R.H.S. of Eq. (39) theoretical expression in the form

$$\chi(s) = \frac{C}{\kappa(s) R_0^3(s)} \tag{59}$$

where

$$\kappa^4(s) = \frac{1}{2\pi} \int_a^b dx \sqrt{(x^2 - a^2)(b^2 - x^2)[(a+b)^2 - x^2]}, \tag{60}$$

$$a = 2m_N, \quad b = \sqrt{2s + m_N^2} - m_N.$$

It can be proved that $\kappa(s)$ has the following asymptotics[6]

$$\kappa(s) \sim \sqrt{s}, \quad s \to \infty,$$

$$\kappa(s) \sim \sqrt{s - 4m_N^2}, \quad s \to 4m_N^2.$$

We used at the moment the simplest function staying in the R.H.S. of Eq. (55) which described these two asymptotics.

Our fit yielded

$$d_1 = (-12.12 \pm 1.023)GeV, \quad d_2 = (89.98 \pm 15.67)GeV^2,$$

$$d_3 = (-110.51 \pm 21.60)GeV^3, \quad c = (6.655 \pm 1.834)GeV^{-2}. \qquad (61)$$

The fitting curve is shown in Figs. 5, 6.

The experimental data on proton-proton total cross-sections display a more complex structure at low energies than the proton-antiproton ones. To describe this complex structure we, of course, have to modify formula (55) without destroying the general structure given by Eq. (39). The modified formula looks like

$$\sigma_{pp}^{tot}(s) = \sigma_{asmpt}^{tot}(s) \times$$

$$\left[1 + \left(\frac{c_1}{\sqrt{s - 4m_N^2} R_0^3(s)} - \frac{c_2}{\sqrt{s - s_{thr}} R_0^3(s)}\right)(1 + d(s)) + Resn(s)\right], \quad (62)$$

where $\sigma_{asmpt}^{tot}(s)$ is the same as in proton-antiproton case (Eq. (57)) and

$$d(s) = \sum_{k=1}^{8} \frac{d_k}{s^{k/2}}, \quad Resn(s) = \sum_{i=1}^{8} \frac{C_R^i s_R^i {\Gamma_R^i}^2}{\sqrt{s(s - 4m_N^2)}[(s - s_R^i)^2 + s_R^i {\Gamma_R^i}^2]}. \quad (63)$$

Compared to Eq. (55) we introduced here an additional term $Resn(s)$ describing diproton resonances which have been extracted from [27, 28]. The positions of resonances and their widths are listed in Table I. The $c_1, c_2, s_{thr}, d_i, C_R^i (i = 1, ..., 8)$ were considered as free fit parameters. The fitted parameters obtained by fit are listed below (see C_R^i in Table I.)

$$c_1 = (192.85 \pm 1.68)GeV^-2, \quad c_2 = (186.02 \pm 1.67)GeV^-2,$$

[6]Integral in R.H.S. of Eq.(60) can be expressed in terms of the Appell function.

$$s_{thr} = (3.5283 \pm 0.0052) GeV^2,$$

$$d_1 = (-2.197 \pm 1.134) 10^2 GeV, \quad d_2 = (4.697 \pm 2.537) 10^3 GeV^2,$$

$$d_3 = (-4.825 \pm 2.674) 10^4 GeV^3, \quad d_4 = (28.23 \pm 15.99) 10^4 GeV^4,$$

$$d_5 = (-98.81 \pm 57.06) 10^4 GeV^5, \quad d_6 = (204.5 \pm 120.2) 10^4 GeV^6,$$

$$d_7 = (-230.2 \pm 137.3) 10^4 GeV^7, \quad d_8 = (108.26 \pm 65.44) 10^4 GeV^8. \qquad (64)$$

The fitting curve is shown in Figs. 7-10. It should be pointed out that our fit revealed that the resonance with the mass $m_R = 2106\, MeV$ should be odd parity. Our fit indicates that this resonance is strongly confirmed by the set of experimental data on proton-proton total cross-sections. That is why a further study of diproton resonances is very desirable.

The figures 4-11 display a very good correspondence of theoretical formula (39) to the existing experimental data on proton-proton and proton-antiproton total cross-sections.

I'd like to emphasize the following attractive features of formula (39). This formula represents hadronic total cross-section in a factorized form. One factor describes high-energy asymptotics of total cross-section and it has the universal energy dependence predicted by the Froissart theorem. Other factor is responsible for the behaviour of total cross-section at low energies and this factor has also a universal asymptotics at the elastic threshold. It is a remarkable fact that the low-energy asymptotics of total cross-section at the elastic threshold is dictated by the high-energy asymptotics of three-body (three-nucleon in that case) forces. This means that we undoubtedly faced very deep physical phenomena here. The appearance of new threshold $s_{thr} = 3.5283\, GeV^2$ in proton-proton channel, which is near to the elastic threshold, is a nontrivial fact too. It's clear that the difference of two identical terms with different thresholds in the R.H.S. of Eq. (62) is a tail of crossing symmetry which was not actually taken into account in our consideration. What physical entity does this new threshold correspond to? This interesting question is still open.

Anyway we have established that simple theoretical formula (39) described the global structure of pp and $p\bar{p}$ total cross-sections in the whole range of energies available up today. Of course, our results concerning a global description of hadronic total cross-sections are to be considered as preliminary ones. We know the ways how they can be refined later on.

7 On the slope of diffraction cone in single diffraction dissociation

We have shown above that the slope of diffraction cone in the single diffraction dissociation is related to the effective interaction radius for three-body forces

$$b_{SD}(s, M_X^2) = \frac{1}{2} R_0^2(\bar{s}, s_0'), \tag{65}$$

$$\bar{s} = 2(s + M_N^2) - M_X^2, \quad s_0' = 2s_0.$$

Let us define the slope of diffraction cone in the single diffraction dissociation at a fixed point over the missing mass

$$B^{sd}(s) = b_{SD}(s, M_X^2)|_{M_X^2 = 2M_N^2}. \tag{66}$$

Now taking into account Eqs. (40,41) where the effective interaction radius for three-body forces can be extracted from

$$R_0^2(2s, 2s_0) = R_0^2(s, s_0) = \frac{1}{2\pi}\sigma^{tot}(s) - B^{el}(s), \tag{67}$$

and the equation

$$\sigma^{el}(s) = \frac{{\sigma^{tot}}^2(s)}{16\pi B^{el}(s)}, \quad (\rho = 0) \tag{68}$$

we come to the fundamental relation between the slopes in the single diffraction dissociation and elastic scattering

$$\boxed{B^{sd}(s) = B^{el}(s)\left(4X - \frac{1}{2}\right)}, \tag{69}$$

where

$$X \equiv \frac{\sigma^{el}(s)}{\sigma^{tot}(s)}. \tag{70}$$

The quantity X has a clear physical meaning, it has been introduced in the papers of C.N. Yang and his collaborators [29, 30].

We found $X = 0.25$ at $\sqrt{s} = 1800\, GeV$ (see the CDF paper mentioned in Introduction). Hence, in that case we have $B^{sd} = B^{el}/2$ which is confirmed not so badly in the experimental measurements.

In the limit of the black disk ($X = 1/2$) we obtain

$$\boxed{B^{sd} = \frac{3}{2} B^{el}}, \tag{71}$$

and

$$\boxed{B^{sd} = B^{el}, \quad at \quad X = \frac{3}{8} = 0.375}. \tag{72}$$

So, we observe that there is quite a nontrivial dynamics in the slopes of diffraction cone in the single diffraction dissociation and elastic scattering processes. In particular, we can study an intriguing question on the black disk limit not only in the measurements of total hadronic cross-sections compared with elastic ones but in the measurements of the slopes in single diffraction dissociation processes together with elastic scattering ones.

There is a more general formula which can be derived with account of the real parts for the amplitudes. This formula looks like

$$\boxed{B^{sd}(s) = B^{el}(s) \left(4X \frac{1 - \rho_{el}(s)\rho_0(s)}{1 + \rho^2_{el}(s)} - \frac{1}{2} \right)}. \tag{73}$$

If $\rho_{el} = 0$ or $\rho_0 = -\rho_{el}$, then we come to Eq. (69). In the case when $\rho_{el} \neq 0$, we can rewrite Eq. (73) in the form

$$\rho_0 = \frac{1}{\rho_{el}} \left[1 - \frac{1 + \rho^2_{el}}{8X} \left(1 + \frac{2B^{sd}}{B^{el}} \right) \right]. \tag{74}$$

Eq. (74) can be used for the calculation of the new quantity ρ_0. Anyway, the measurements of real parts for the amplitudes seem to play an important role in the future high energy hadronic physics.

8 On total single diffractive dissociation cross-section

For the total single diffractive dissociation cross-section defined as

$$\sigma_{sd}(s) = 2\pi \int_{M^2_{min}}^{0.1s} \frac{dM^2_X}{s} \int_{t_-(M^2_X)}^{t_+(M^2_X)} dt A(s, M^2_X) \exp[b(s, M^2_X)t] \tag{75}$$

we obtained the following asymptotic formula

$$\sigma_{sd}(s) = \frac{A_0 + A_2 \ln^2(\sqrt{s}/\sqrt{s_0})}{c_0 + c_2 \ln^2(\sqrt{s}/\sqrt{s_0})}, \tag{76}$$

where c_0, c_2 are related to effective interaction radius for three-body forces

$$R_0^2(s) = c_0 + c_2 \ln^2(\sqrt{s}/\sqrt{s_0}),$$

and A_0, A_2 to be found from the fit to the experimental data on σ_{sd}. The experimental values for $p\bar{p}$ single diffraction dissociation cross-sections, which were used, are listed in Table II. Our fit yielded [26, 31]

$$A_0 = 23.395 \pm 2.664\, mbGeV^{-2}, \quad A_2 = 4.91 \pm 0.26\, mbGeV^{-2}.$$

The fit result is shown in Fig. 11. As you can see, the fitting curve goes excellently over the experimental points of the CDF group at Fermilab.

Thus, we have shown that from the generalized asymptotic theorems a là Froissart there follows a simple formula which allows one to match the experimental data on $p\bar{p}$ single diffraction dissociation cross-sections at high energies including lower energies as well. At present only the suggested approach allows one to quantitatively describe the observed behaviour of $p\bar{p}$ single diffraction dissociation cross-sections.

Some time ago many high energy physicists thought that the increase of total cross-sections was due to the same increase of single diffraction dissociation cross-sections. Now we know that this thought is wrong and, moreover, we understand why this is the case.

As it has been shown above the phenomenon of exceedingly moderate energy dependence of single diffraction dissociation cross-sections on s observed by CDF at Fermilab is a manifestation of unitarity saturation of three-nucleon forces at Fermilab Tevatron energies. This phenomenon is confirmed in the dynamics consistent with unitarity becoming apparent in the effect of screening of three-body forces by two-body ones. It is to be compared with the discovery of the increase of pp total cross-sections at CERN ISR and of the growth of K^+p total cross-sections revealed at Serpukhov accelerator. In this context, the CDF data are the ones of the most significant experimental results obtained in the last years.

In fact, we have found the bound (like Froissart bound!)

$$\boxed{\sigma_{sd}(s) < Const, \quad s \to \infty}. \tag{77}$$

I'd like especially to point out that analyticity and unitarity together with the dynamic apparatus of single-time formalism in QFT provide the clear answers to the asymptotic behaviour both the elastic scattering and single diffraction dissociation at high energies, which correspond to the experimentally observable picture.

It is very nice that the understanding of "soft" physics based on general principles of QFT, such as analyticity and unitarity, is so fine confirmed by the experimentally observable picture compared to the models where the general principles have been broken down.

I hope that it will be possible to test the obtained results at higher energies, such as those of the LHC collider and even higher ones.

9 On the forms of strong interaction dynamics

Conditionally there are two forms of strong interaction dynamics: t-channel form and s-channel one.

t-channel form

The fundamental quantity here is some set of Regge trajectories:

$$t-channel form \qquad \Longleftrightarrow \qquad \alpha_R(t). \tag{78}$$

Here subscript R enumerates different Regge trajectories which are the poles in the t-channel partial wave amplitudes for the given process. There are a lot of people who work in the field of t-channel dynamics of strong interactions.

Some part of scientific community works in the field of s-channel form of strong interaction dynamics.

s-channel form

The fundamental quantity here is an effective interaction radius of fundamental forces:

$$s-channel form \qquad \Longleftrightarrow \qquad R_\alpha(s). \tag{79}$$

Here subscript α enumerates different types of hadrons and fundamental forces acting between them. The s-channel form of dynamics allows one to create a physically transparent and visual geometric picture of strong

interactions for hadrons. I'd like to emphasize the attractive features of this form of strong interaction dynamics.

- Universality (existence of pion with $m_\pi \neq 0$):

$$\boxed{R_\alpha(s) \sim \frac{r_\alpha}{m_\pi} \ln \frac{s}{s_0}, \quad s \to \infty}.$$

- Compatibility with the general principles of relativistic quantum theory.
- Fine mathematical structures are given by the global analyticity together with single-time formalism in QFT.

That is why, in our opinion, the s-channel form of strong interaction dynamics is more preferable than the t-channel one.

10 Conclusion

In Commemoration of the 200th Anniversary of Alexander S. Pushkin I'd like to conclude my talk with the Ode:

To learn or not to learn?
Of course to learn to be The Forces,
To be The Three-Body Forces as well,
But not Номер-Он *alone.*
That is a sound of Bell!...

Acknowledgements

It is my pleasure to express thanks to the Organizing Committee for the given opportunity to attend the VIIIth Blois Workshop and present the report there. I am indebted to V.V. Ezhela for the access to the computer readable files on total proton-proton and proton-antiproton cross-sections in the IHEP COMPAS database. The friendly encouragement and many pieces of good advice on computer usage from A.V. Razumov are gratefully acknowledged.

References

[1] F. Abe et al., (CDF) Phys. Rev. D**50**, 5535 (1994).

[2] A.M. Cooper-Sarkar et al., Preprint DESY 97-226, hep-ph/9712301.

[3] K. Goulianos, J. Montanha, Phys. Rev. D**59**, 114017 (1999); eprint hep-ph/9805496.

[4] E. Gostman, E.M. Levin, U. Maor, Phys. Rev. D**49**, R4321 (1994).

[5] E.S. Martynov, B.V. Struminsky, in: *Proceedings of the XIth Workshop on "soft" physics HADRONS-95, Novy Svet, 1995,* eds. G. Bugrij, L. Jenkovsky, E. Martynov (Kiev, 1995), p.53-60; Phys. Rev. D**53**, 1018 (1996); Sov. J. Yad. Phys. **59**, 1817 (1996).

[6] Proceedings of the Workshop on *QUANTUM INFRARED PHYSICS*, 6-10 June 1994, The American University of Paris, eds. H.M. Freid, B. Muller, World Scientific Singapore, New Jercey, London, Hong Kong.

[7] M.L. Good, W.D Walker, Phys. Rev. **120**, 1857 (1960).

[8] E.M. Levin, Everything about Reggeons, hep-ph/9710546.

[9] V.S. Fadin, E.A. Kuraev, L.N. Lipatov, Phys. Lett. B**60**, 50 (1975); E.A. Kuraev, L.N. Lipatov, V.S. Fadin, Zh. Eksp. Teor. Fiz. **71**, 840 (1976)[Sov. J. JETP **44**, 443 (1976)]; ibid. **72**, 377 (1977)[**45**, 199 (1977)]; Ya.Ya. Balitskii, L.N. Lipatov, Sov. J. Nucl. Phys. **28**, 822 (1978).

[10] A. Donnachie, P.V. Landshoff, Z. Phys. C**2**, 55 (1979); Phys. Lett. B**123**, 345 (1983); Nucl. Phys. B**231**, 189 (1984); Nucl. Phys. B**244**, 322 (1984).

[11] J.D. Bjorken, Nucl. Phys.(Proc. Suppl.) B**25**, 253 (1992).

[12] A.A. Arkhipov, preprint IHEP 96-66, Protvino, 1996; in: *Proceedings of the XIIth Workshop on "soft" physics HADRONS-96, Novy Svet, 1996,* eds. G. Bugrij, L. Jenkovsky, E. Martynov (Kiev, 1996), p. 252-263.

[13] N.N. Bogoljubov, A.A. Logunov, I.T. Todorov, A.I. Oksak. General Principles of Quantum Field Theory, Moscow, Nauka, 1987.

[14] A.A. Arkhipov, Sov. J. Theor. Math. Phys. **83**, 247 (1990).

[15] A.A. Arkhipov, V.I. Savrin, Sov. J. Theor. Math. Phys. **16**, 328 (1973); **19**, 320 (1974); **24**, 78 (1975); **24**, 303 (1975).

[16] A.A. Arkhipov, V.I. Savrin, Sov. J. Theor. Math. Phys. **49**, 3 (1981).

[17] A.A. Arkhipov, Rep. on Math. Phys. **20**, 303 (1984).

[18] H. Lehman, Nuovo Cim. **10**, 579 (1958); Nuovo Cimento Suppl. **14**, 153 (1959).

[19] O.W. Greenberg, F.E. Low, Phys. Rev. **124**, 2047 (1961).

[20] A. Martin, Phys. Rev. **129**, 1432 (1963); Nuovo Cim. **42A**, 930 (1966); **44A**, 1219 (1966).

[21] G. Sommer, Nuovo Cim. **48A**, 92 (1967), **52A**, 373 (1967), **52A**, 850 (1967), **52A**, 866 (1967).

[22] A.A. Logunov, Nguyen Van Hieu, O.A. Khrustalev, in: Problems of Theoretical Physics, Essays dedicated to Nikolai N. Bogoljubov on the occasion of his sixtieth birthday, Publishing House Nauka, Moscow, 1969, p. 90.

[23] M. Froissart, Phys. Rev. **123**, 1053 (1961).

[24] A.A. Arkhipov, V.I. Savrin, Sov. J. Theor. Math. Phys. **24**, 78 (1975).

[25] A.A. Arkhipov, Sov. J. Theor. Math. Phys. **49**, 320 (1981).

[26] A.A. Arkhipov, P.M. Nadolsky, preprint IHEP 97-6, Protvino, 1997.

[27] Yu.A. Troyan, V.N. Pechenov, Sov. J. Yad. Phys. **56**, 191 (1993).

[28] Yu.A. Troyan, Sov. J. Physics of Element. Part. and Atomic Nuclei **24**, 683 (1993).

[29] A.W. Chao, C.N. Yang, Phys. Rev. D**8**, 2033 (1973).

[30] T.T. Chou, C.N. Yang, Phys. Lett. B**128**, 457 (1983).

[31] A.A. Arkhipov, Single Diffractive Dissociation in $p\bar{p}$ Collisions at High Energy - Talk Presented at "Workshop on Diffractive Physics, LAFEX International School on High Energy Physics (LISHEP-98), Rio de Janeiro, 16 - 20 February, 1998."

[32] B.E. Ansorge et al., Z. Phys. C**33**, 175 (1986).

[33] G.J. Alner et al., (UA5) Phys. Rep. **154**, 247 (1987).

[34] D. Bernard et al., (UA4) Phys. Lett. B**186**, 227 (1987).

[35] N.A. Amos et al., (E710) Phys. Lett. B**243**, 158 (1990); N.A. Amos et al., (E710) Phys. Lett. B**301**, 313 (1993).

[36] R.M. Baltrusaitis et al. (Fly's Eye Collaboration), Phys. Rev. Lett. **52**, 1380 (1984).

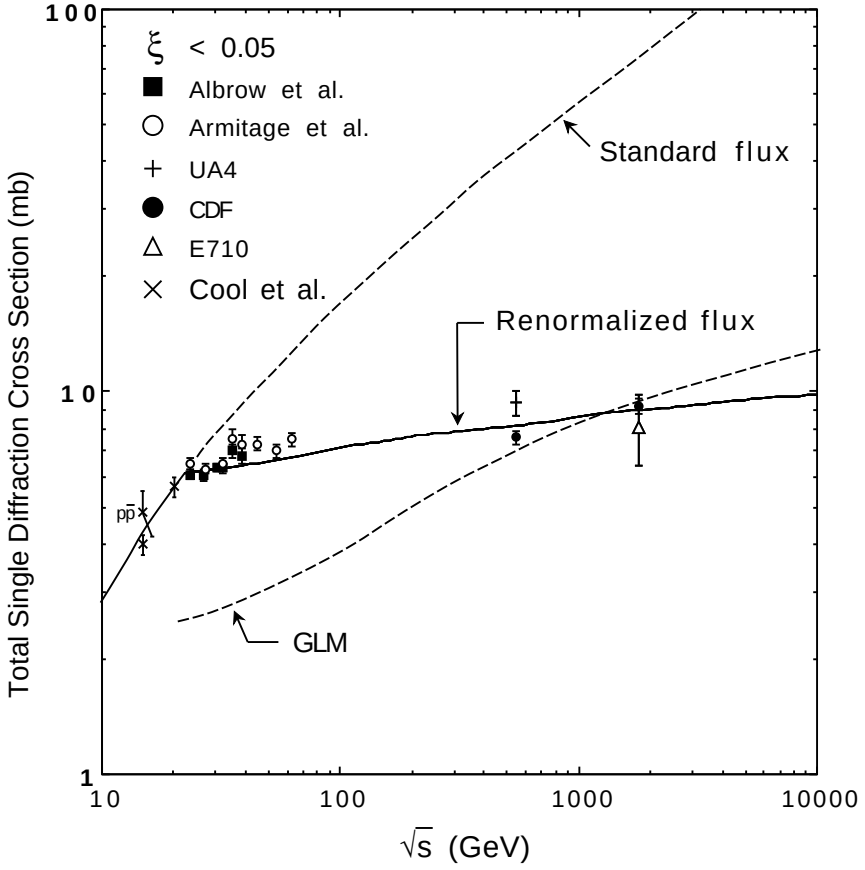

Figure 1: The total single diffraction cross-sections for $p(\bar{p})+p \to p(\bar{p})+X$ vs $\sqrt{s}$ compared with the predictions of the renormalized Pomeron flux model of Goulianos [3] (solid line) and of the model Gostman, Levin and Maor [4] (dashed line, labelled GLM).

$$\frac{s}{\pi}\frac{d\sigma_{hN\to NX}}{dtdM_X^2} = \frac{(2\pi)^3}{I(s)}\chi(\bar{s})Im\mathcal{F}_0(\bar{s};-\vec{\Delta},\vec{\Delta},\vec{q};\vec{\Delta},-\vec{\Delta},\vec{q})$$

$$\bar{s} = 2(s+M_N^2) - M_X^2, \quad t = -4\vec{\Delta}^2.$$

$$(I(s)/\chi(\bar{s}) - \text{"renormalized flux"!})$$

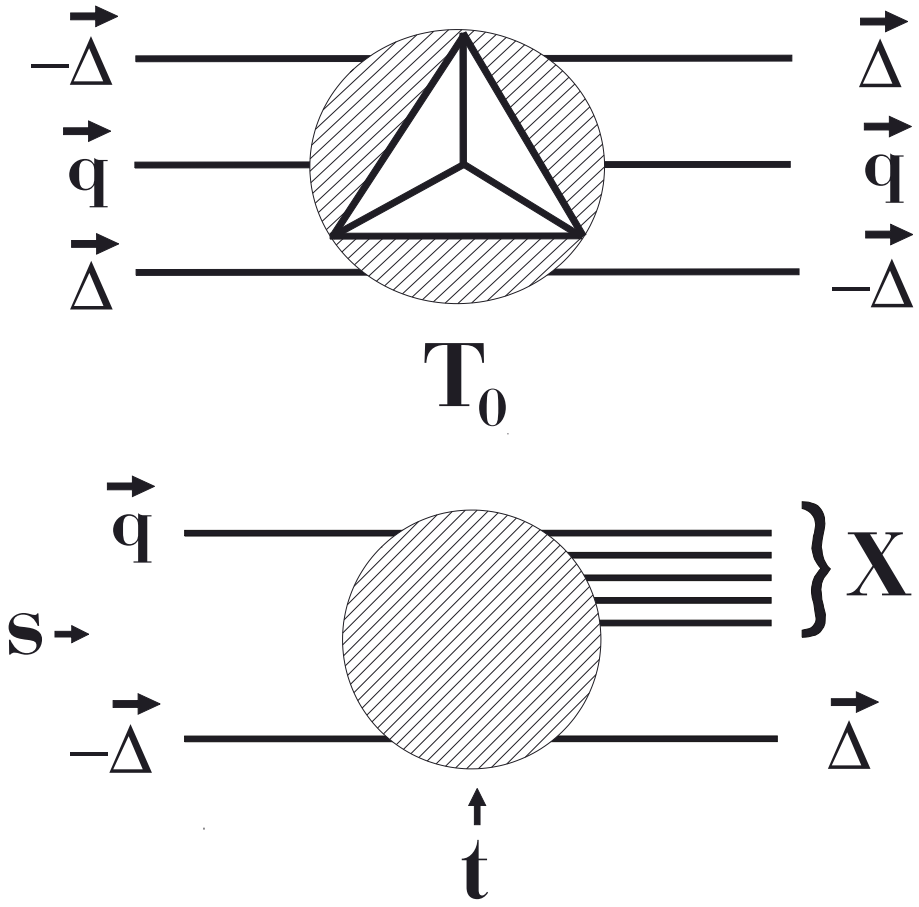

Figure 2: Kinematical notations and configuration of momenta in the relation of one-particle inclusive cross-section to the three-body forces scattering amplitude.

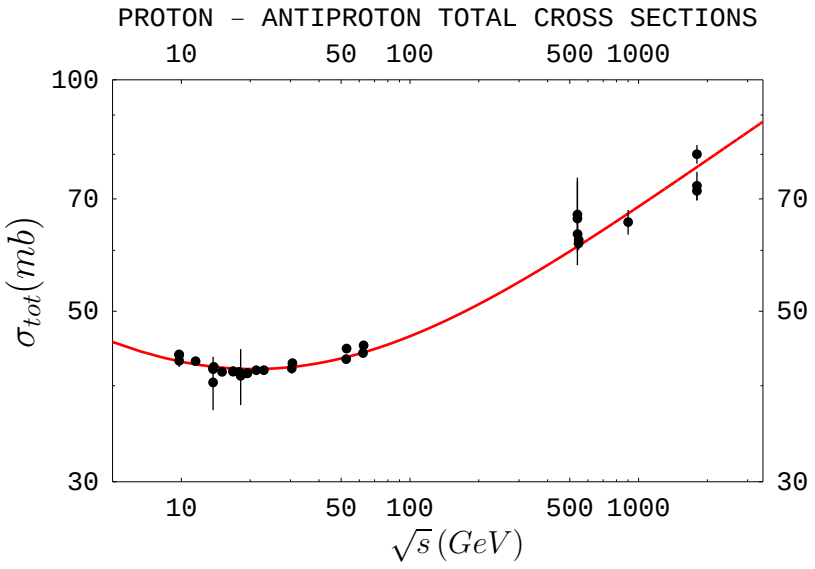

Figure 3: The total proton-antiproton cross-section versus $\sqrt{s}$ compared with formula (50). Solid line represents our fit to the data. Statistical and systematic errors added in quadrature.

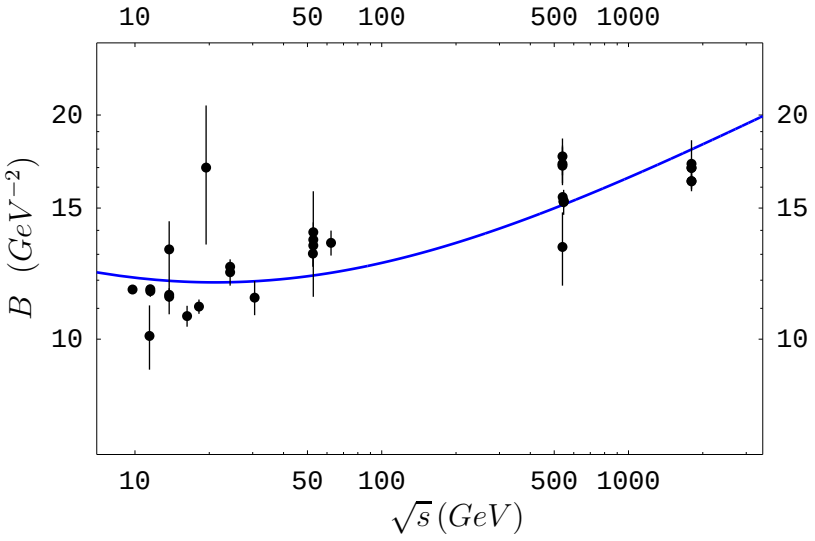

Figure 4: Slope B of diffraction cone in $p\bar{p}$ elastic scattering. Solid line represents our fit to the data.

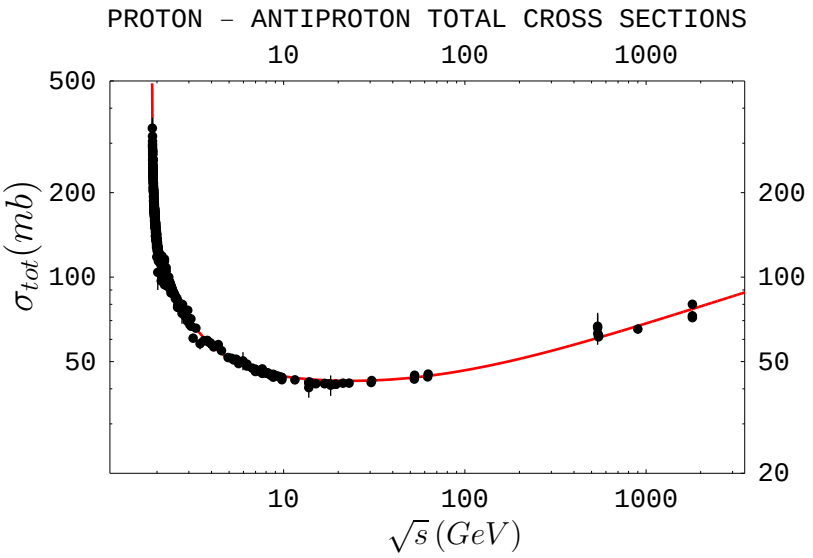

Figure 5: The total proton-antiproton cross-section versus $\sqrt{s}$ compared with formula (55). Solid line represents our fit to the data.

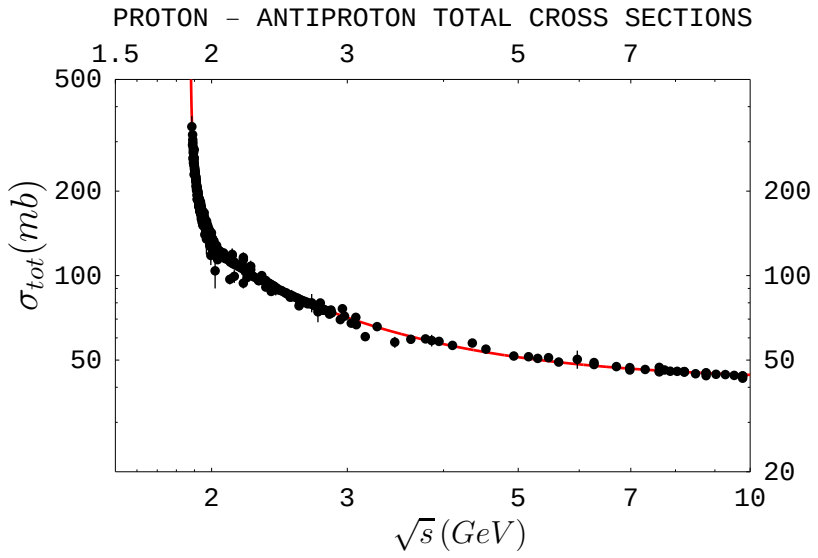

Figure 6: The total proton-antiproton cross-section versus $\sqrt{s}$ compared with formula (55) in the range $\sqrt{s} < 10\,GeV$ (fragment of Fig. 5). Solid line represents our fit to the data.

$m_R(MeV)$	$\Gamma_R(MeV)$	$C_R(GeV^2)$
1937 ± 2	7 ± 2	0.0722 ± 0.0235
1955 ± 2	9 ± 4	0.1942 ± 0.0292
1965 ± 2	6 ± 2	0.1344 ± 0.0117
1980 ± 2	9 ± 2	0.3640 ± 0.0654
2008 ± 3	4 ± 2	0.3234 ± 0.0212
2106 ± 2	11 ± 5	-0.2958 ± 0.0342
2238 ± 3	22 ± 8	0.4951 ± 0.0559
2282 ± 4	24 ± 9	0.0823 ± 0.0319

Table I: Diproton resonances extracted from [27, 28].

$\sqrt{s}\ (GeV)$	$\sigma_{sd}^{pp}(mb)$	References
20	4.9 ± 0.55	[1]
200	4.8 ± 0.9	[32]
546	5.4 ± 1.1	[33]
546	7.89 ± 0.33	[1]
546	9.4 ± 0.7	[34]
900	7.8 ± 1.2	[34]
1800	9.46 ± 0.44	[1]
1800	11.7 ± 2.3	[35]
1800	8.1 ± 1.7	[35]

Table II: Data on $p\bar{p}$ single diffraction dissociation cross-sections.

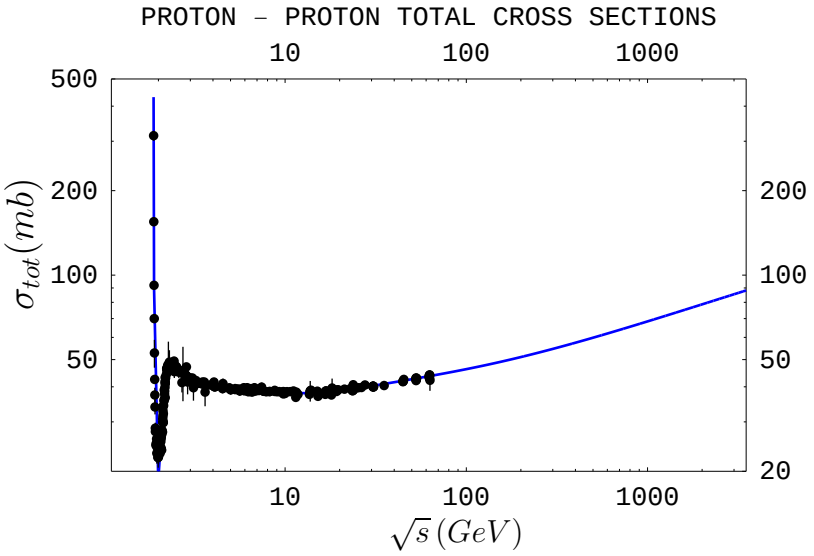

Figure 7: The total proton-proton cross-section versus $\sqrt{s}$ compared with formula (62). Solid line represents our fit to the data. Statistical and systematic errors added in quadrature.

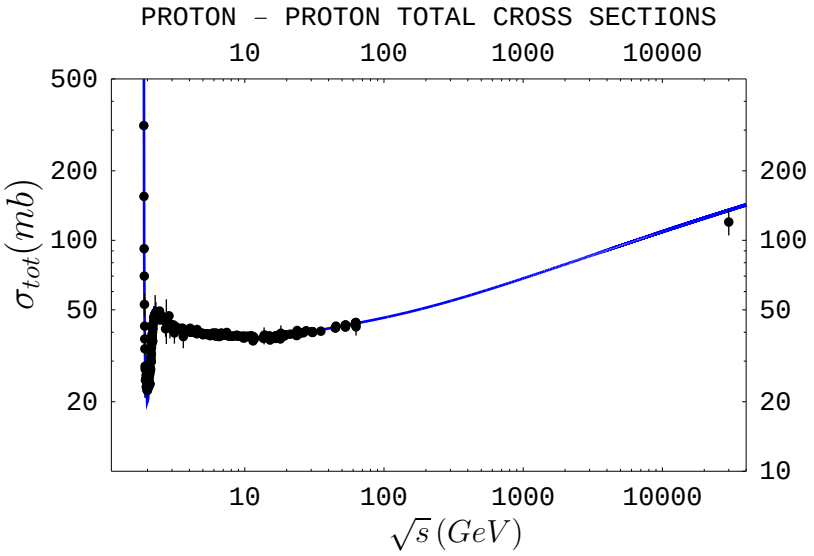

Figure 8: The total proton-proton cross-section (vs $\sqrt{s}$) including a point from cosmic rays experiment [36] compared with formula (62). Solid line represents our fit to the data.

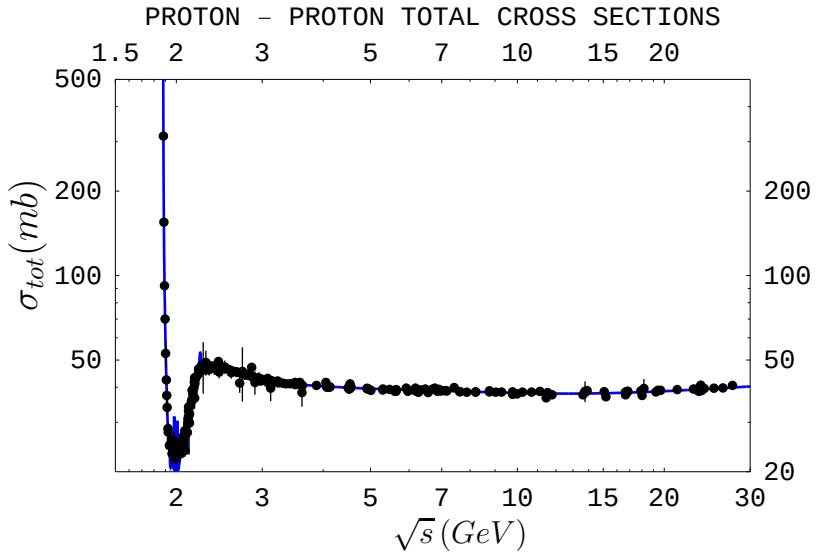

Figure 9: The total proton-proton cross-section in the range $\sqrt{s} < 30\,GeV$ compared with formula (62). Solid line represents our fit to the data.

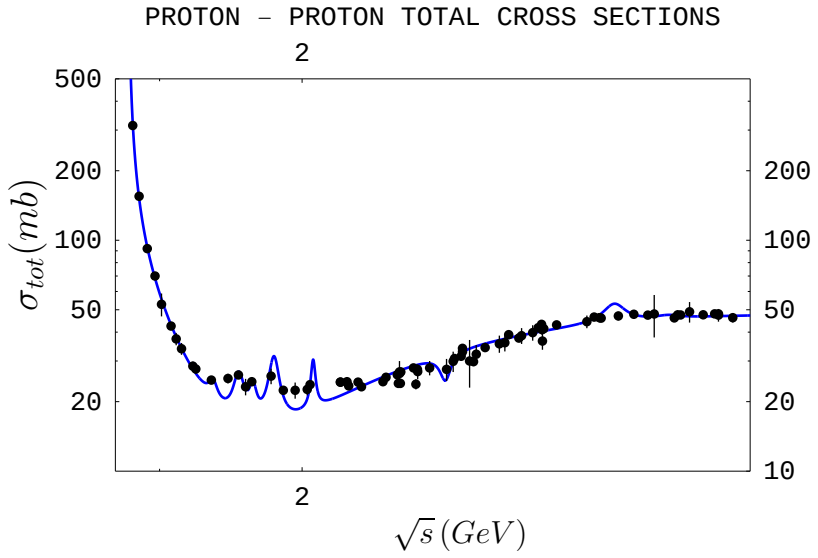

Figure 10: The total proton-proton cross-section at low energies compared with formula (62). Solid line represents our fit to the data.

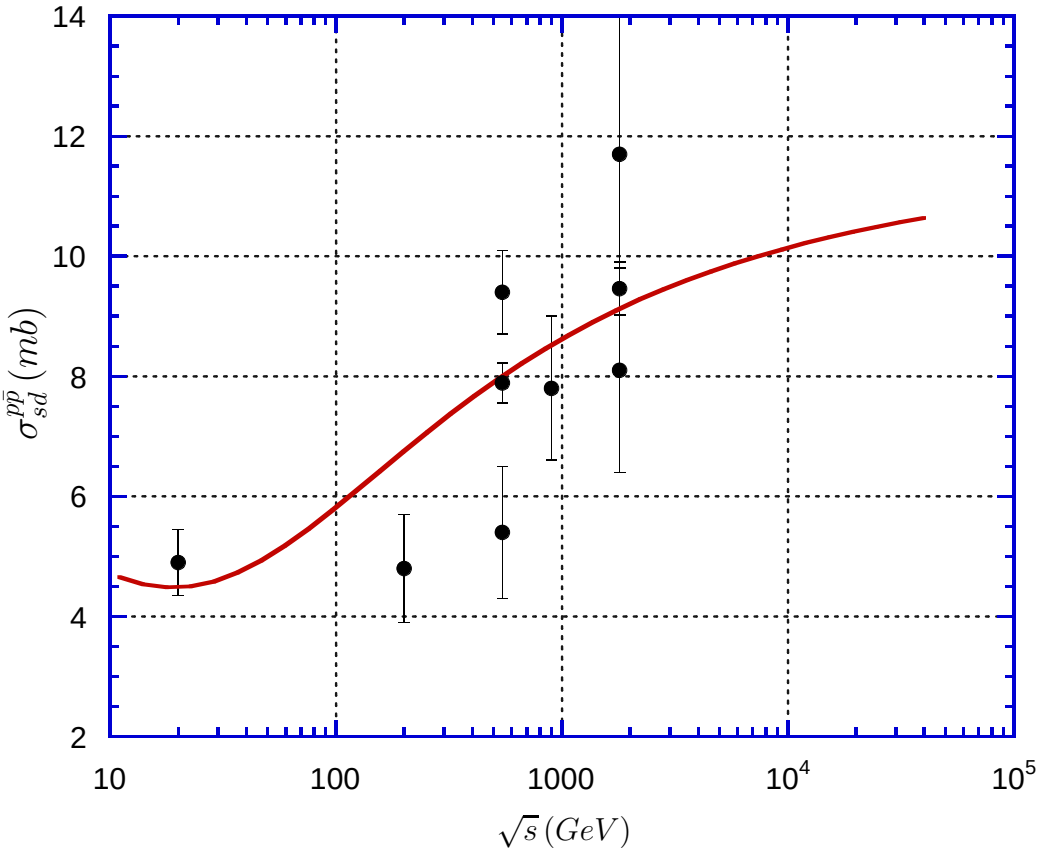

Figure 11: Total single diffraction dissociation cross-section compared with formula (76). Solid line represents our fit to the data.